



Semi-active noise suppression based on SSD technique using piezoelectric elements

Hongli Ji^{1,2}, Li Cheng², Jinhao Qiu¹, and Hong Nie¹

¹State Key Laboratory of Mechanics and Control of Mechanical Structures, Nanjing University of Aeronautics and Astronautics, China

²Department of Mechanical Engineering, The Hong Kong Polytechnic University, Hong Kong, China

ABSTRACT

Noise suppression using piezoelectric elements has received extensive attention in recent years. Traditional active noise control methods usually require the use of microphones as sensors to directly measure the sound pressure in either feed-forward or feedback control schemes. This makes the traditional active noise isolation more difficult to implement in some practical applications. Nonlinear semi-active Synchronized Switch Damping (SSD) approaches are typical switched-voltage control methods, which have recently been a topic of active research in the field of vibration control. In this paper, SSD method is proposed for the suppression of noise transmission through an aluminum panel. In a typical SSD setting, microphones are not required for feedback control, but are used merely as sensors to evaluate the control performance. The layout of the piezoelectric elements on the panel has been optimized based on the mode shape dominating the noise radiation. SSDV (SSD based on voltage sources) was used to improve the control performance. Experimental results show that the proposed control approach exhibits good performance in suppressing noise transmission.

Keywords: Semi-active control; noise suppression; Synchronized switch damping; piezoelectric elements.

1. INTRODUCTION

Suppression of noise transmission has received much attention in recent years because of its practical implication in many engineering structures such as civil aircraft, passenger trains and cars etc. [1-3]. Conventional methods can be roughly categorized into passive, active and semi-active. In passive methods, absorbing materials are used to improve the effectiveness of noise transmission suppression of double-walled structure [4]. Damping layers can also be used to reduce the vibration level of structures, consequently leading to suppression in the noise transmission [5]. However, these methods start to hit their limit in many applications. Further improvement through purely passive means is usually at the expense of increasing cost, structural weight and size.

Active methods for noise transmission suppression using structural vibration control have been proposed owing to the progress in electronic and computer technologies to overcome the disadvantage of passive methods. Studies in the active suppression of noise transmission have been reported [6-12]. Jones and Fuller [6] studied the reduction of interior sound fields in flexible cylinders induced by an exterior acoustic monopole using active vibration control. Results indicated spatially averaged noise reductions of above 20 dB over the source plane for acoustic resonant conditions within the cavity. Koshigoe *et al.* [8] used piezoelectric actuators and a neural network controller in the suppression of noise transmission through a plate structure. Ho *et al.* [9] used a piezoelectric actuator and a velocity feedback controller for the reduction of noise transmission through a plate subject to a white noise excitation using vibration as the feedback signal. Hong *et al.* [10] used a filtered-X LMS algorithm to control the transmission of noise through a rectangular plate, by considering some specific frequencies. A new noise isolation system of a composite board without using external noise sensors such as microphones was constructed by Ji *et al.* [13]. With only one embedded piezoelectric patch in the smart board which functions as both a sensor and an actuator, the system consists of a self-sensing actuator, a neural network identifier and an adaptive feedback controller using Filtered-X LMS algorithm.

Although active methods have the advantages of high control performance and robustness, they also share the drawbacks of requiring high-performance digital signal processors and bulky power amplifiers, which is undesirable in many applications. In order to tackle the problem, several semi-active approaches have been proposed [14-20], among which the pulse switching technique has been receiving much attention in recent years [16-20]. The pulse switching technique consists in a fast inversion of voltage on the piezoelement using a few basic electronics, which is synchronized with the mechanical vibration. In the methods proposed by Richard *et al.* [16], the voltage on the piezoelectric element is switched at the strain extrema or displacement extrema of the vibration, referred to as Synchronized Switch Damping (SSD) techniques. On the other hand, as proposed by Onoda and Makihara [17], the switch can also be actively controlled, referred to as active control theory based switching technique here.

In the SSD technique, the control performance mainly depends on the value of the voltage applied to the piezoelectric elements. Several variations of the SSD control techniques have been proposed in the literature to increase the control performance. To increase the voltage on the piezoelectric actuator, an inductance can be connected to the shunt circuit to invert the voltage. This method is called SSDI. The inversion process boosts the voltage, thus increasing energy dissipation. The objective of all switch control algorithms is to maximize the energy dissipated in each cycle of vibration. To further improve the control performance, a method called SSDV, standing for synchronized switch damping on voltage, has been proposed [18,19]. The SSD technique was originally proposed for vibration damping, but recently it has also been applied to suppression of structural radiation and transmission [18, 21].

In this study, SSD method is applied to suppression of noise transmission through a panel. The microphone is not used as feedback sensor, but to evaluate the control performance. The layout of the piezoelectric elements on the panel has been optimized based on the mode shapes, responsible for noise radiation. SSDV which is based on voltage sources is used to maximize the control performance, which is demonstrated by experimental results.

2. SSD CONTROL METHOD

SSD control was proposed to provide an alternative to the existing active and passive control methods, and hopefully could alleviate some of the existing drawbacks of these methods. In SSD control, the voltage on the piezoelectric actuator is switched synchronously with the vibration of the host structure to achieve enhanced damping effect. The power consumption of the control system is usually low because the main consumption is in the switch circuit. It is also robust because switch actions are synchronized with vibration so that it can automatically trace the frequency of structural vibration.

With a piezoelectric actuator bonded on a host vibrating structure, a voltage is generated on it in the open-circuit state by the mechanical strain, which is proportional to the deformation of piezo-element. Though mechanical energy is converted to electrical energy as the strain increases, electrical energy is converted back to mechanical energy as the strain decreases. Hence there is no net energy conversion in a full cycle of mechanical vibration. If the voltage on the piezoelectric actuator is processed by a switch circuit by shifting its phase, its amplitude can be magnified. Hence net energy conversion from mechanical to electrical is produced, resulting in an equivalent added damping effect to the host structure. A typical switch circuit for SSDV method is shown in Fig. 1(a) and the corresponding actuator voltage is shown in Fig. 1(b).

In the absence of voltage sources in the circuit, the scheme becomes the switch circuit of SSDI control. Between the actuator voltages V_M and V_m , there exist the following relationships [22]:

$$V_m = \gamma V_M + (1 + \gamma) V_{cc} \quad \text{and} \quad V_M = V_m + 2\alpha u_M / C_p \quad (1)$$

where $\gamma \in [0,1]$ is the voltage inversion coefficient and u_M is the maximum amplitude of vibration displacement. The inversion coefficient γ is a function of the quality factor of the shunt circuit, Q_c :

$$\gamma = e^{-\pi/2Q_c} \quad (2)$$

The following switched voltage can be obtained [23]:

$$V_{sw} = \frac{1}{2}(V_M + V_m) = \frac{1+\gamma}{1-\gamma} \left(\frac{\alpha}{C_p} u_M + V_{cc} \right) \quad (3)$$

The switched voltage can be effectively raised by increasing the output of the voltage source V_{cc} .

The switched voltage generates a control force, which has opposite direction with respect to vibration velocity so that mechanical energy is always converted to electrical energy. In steady-state control, the converted energy in a cycle of vibration can be expressed as

$$\int_0^T \alpha V_a \dot{u} dt = 4\alpha V_{sw} u_M \quad (4)$$

where T is the period of mechanical vibration.

The above expression indicates that the converted energy is proportional to the amplitude of converted voltage. Inclusion of a voltage source in the switch circuit will increase the amplitude of switched voltage and consequently improve the control performance.

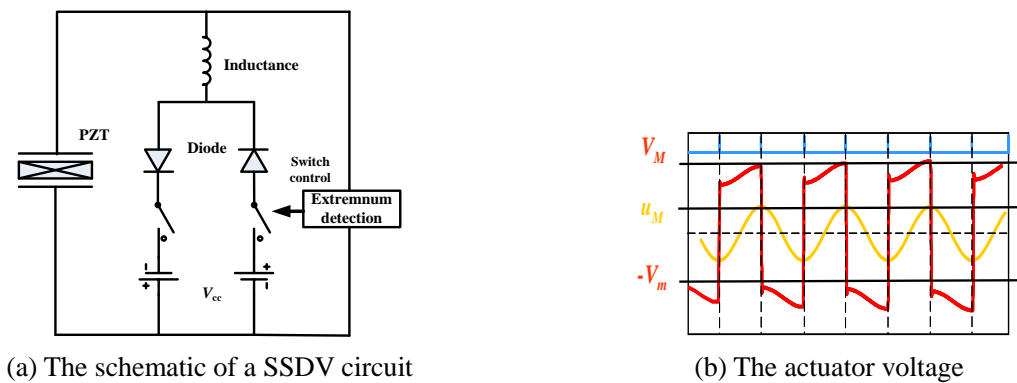


Figure 1 – The principle of SSDV

3. EXPERIMENT SETUP AND CONDITIONS

The panel used in this study was an aluminum plate of 1 mm thick and 480 mm × 480 mm large. The four edges of the panel were clamped on a box using a rigid aluminum frame as shown in Figure 2, producing an effective vibrating area of 420 mm × 420 mm. The walls of the box were made of PMMA (polymethy methacrylate), which could provide more than 30dB sound isolation in the frequency band of interest below 1 kHz.

The material properties of the panel are tabulated in Table 1. Five piezoelectric patches, used as actuators, were bonded on the surface of the panel, with locations shown in Figures 3 and 4. The one at the center has larger size (40 mm × 40 mm) than the four others (30 mm × 30 mm) around it. Their geometrical and material parameters are shown in Tables 2. The five piezoelectric patches are divided into two sets: the one at the center in one set and the other four in the other set. The four piezoelectric patches in the second set are switched by the same switch in a synchronized way. A 6.5 inch loudspeaker inside the box was used to generate noise and an accelerometer shown by a circular mark in Figure 3 was used to measure the vibration of the panel. A microphone installed at 0.4 m away from the center of the plate was used to monitor the sound pressure outside the box, inside a full anechoic chamber, as shown in Figure 2. The schematic of the control system is shown in Figure 4. A source signal from the signal generator was amplified and applied to the loudspeaker to generate noise inside the cavity. The noise transmitted through the panel was measured by the microphone. The source signal can be a pure tone of specific frequency, or a combination of two harmonic signals. The two sets of piezoelectric patches were switched independently by two switch circuits. The signal from the accelerometer was used for switch control as shown in Figure 4. In two-mode control, an observer was used to separate the modal information of the two dominant modes.



Figure 2 – Experimental setup

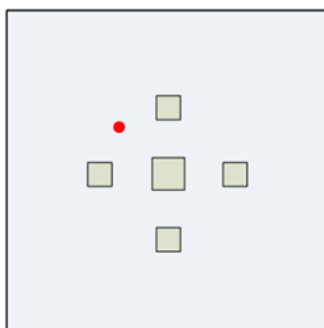


Figure 3 – Distribution of piezoelectric patches and accelerometer

Table 1 – Parameters of the panel

Components	Parameters
Actual volume of the cavity	420 mm × 420 mm × 365 mm
Thickness of the aluminum	1 mm
Dimensions of the outer frame	480 mm × 480 mm
Dimensions of the inner frame	420 mm × 420 mm
Thickness of the PMMA	50 mm
Poisson ratio of the aluminum	0.33
Young's module of the aluminum	70 GPa
Density of the aluminum	2700 kg/m ³

Table 2 – Parameters of the PZT patches

Properties	PZT-PMN-51
Poisson ratio	0.39
Density	7600 [kg/m ³]
Thickness	1 × 10 ⁻³ [m]
Piezoelectric constant d_{31}	-270 × 10 ⁻¹² [c/N]

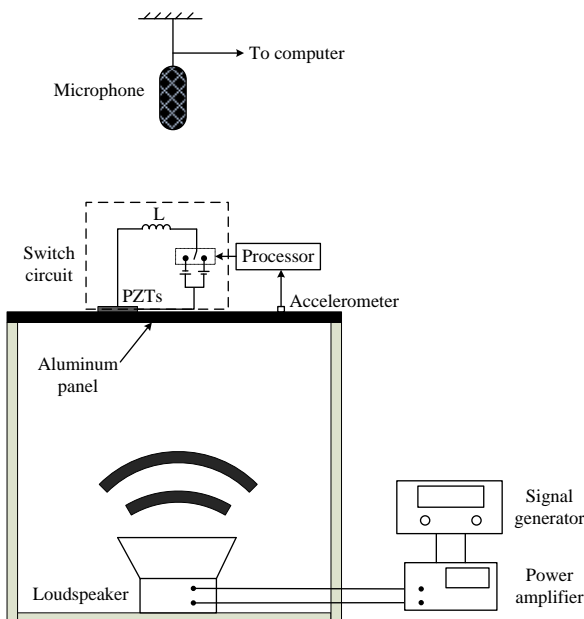


Figure 4 –A schematic of the control system

4. CHARACTERISTICS OF VIBRATION AND NOISE TRANSMISSION

The dynamics of the panel were shown by the measured frequency response function using the accelerometer under sweeping frequency excitation by the speaker inside the box, shown in Figure 5. Figure 6 shows the spectrum of the sound pressure measured by the microphone under a white noise excitation within the same frequency band.

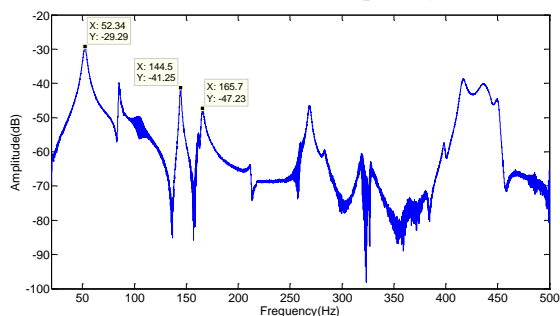


Figure 5 – Frequency response of the panel under sweeping frequency excitation

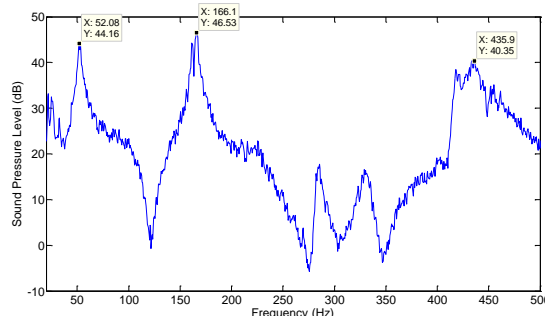


Figure 6 – Spectrum of the sound pressure level

It can be seen that the panel exhibits rather complex dynamics, evidenced by a number of resonance peaks. Due to the symmetrical acoustic excitation, however, only a few modes contribute to the sound radiation. More specifically, the two peak frequencies of the noise spectrum at 52 Hz and 166 Hz correspond to two structural resonances (1st and 5th modes of the panel). Simulated mode shapes of these two modes are shown in Figure 7.

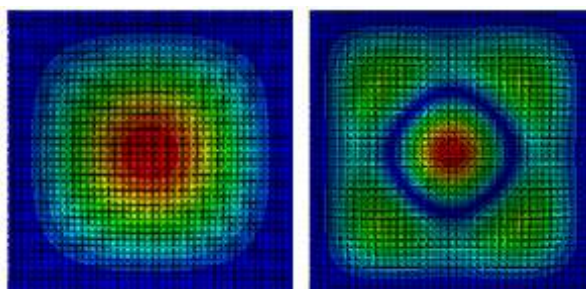


Figure 7 – Shape of the 1st and 5th modes of the panel (simulation result)

5. CONTROL RESULTS AND ANALYSES

5.1 Single-Mode Control

In the single-mode control experiment, the panel was excited by a pure tone at one of the resonance frequencies. The solid line in Figure 8 shows the spectrum of sound pressure level in the frequency range from 20 Hz to 500 Hz when panel was excited at the first resonance frequency of 52 Hz. The peak at this frequency is dominant, but there is also a peak at the double frequency. When semi-active control is deployed, the dominant peak at 52 Hz is reduced from 55.4 dB to 47.9 dB, as shown in Fig. 8. Figure 9 shows the sound pressure variation in the time domain. The amplitude of sound pressure was reduced significantly after control. However, the spectrum in Fig.8 also shows that a few spikes were also produced at the high-order harmonic frequencies. Analysis shows that the control voltage of SSD control (shown in Figure 10) contains a rectangular wave, which consists of the fundamental harmonic and high-order harmonic components. This is probably due to the imperfection of the circuit design, such producing an obvious signal saturation of the control voltage. The high-order components in the controlled structured can be reduced considerably by increasing the voltage inversion time. Figure 11 shows the control result when a parallel capacitor of 3 μ F is connected to the piezoelectric element to increase the voltage inversion time. Figure 12 shows the corresponding voltage on the piezoelectric actuator. It can be seen that the control performance is significant improved, evidenced by a reduction of the second harmonic noise. In what follows, a parallel capacitor of 3 μ F is connected to the piezoelectric element to increase the voltage inversion time.

To evaluate the overall control performance quantitatively, the overall sound pressure level L_p was calculated by integrating the spectrum from 20 Hz to 500 Hz. In the single-mode control at 52 Hz, the peak value was reduced by 11.33 dB and the attenuation of overall sound pressure level was 9.93 dB.

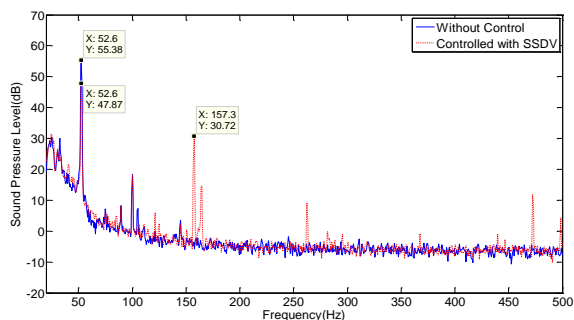


Figure 8 – Spectrum of sound pressure level

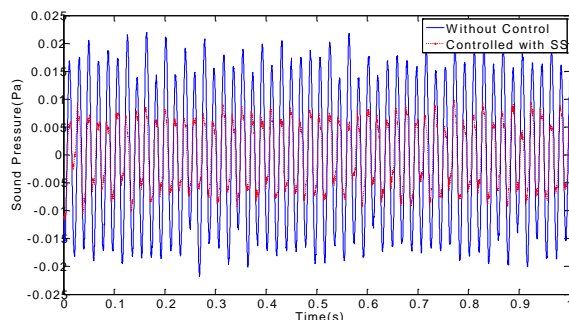


Figure 9 – Sound pressure in time domain

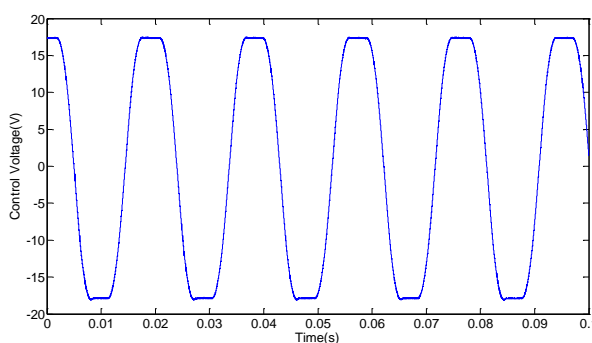


Figure 10 – Voltage on the piezoelectric actuator

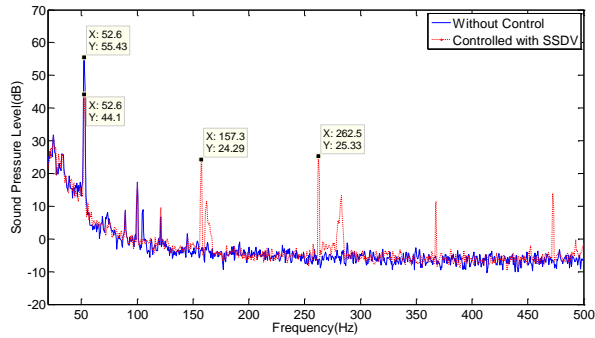


Figure 11 – Spectrum of sound pressure level when a parallel capacitor of 3 μ F is connected to PZT

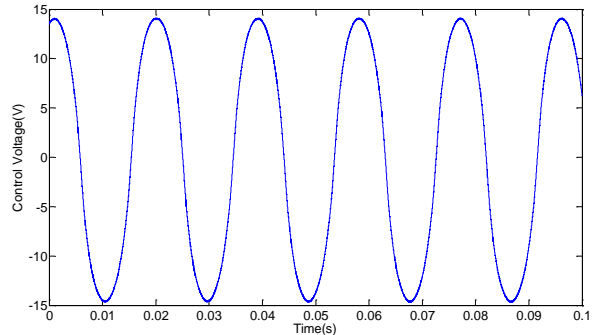


Figure 12 – Voltage on the piezoelectric actuator

Experiment was also conducted at 166 Hz. The solid line in Figure 13 shows the spectrum of sound pressure level when panel is excited at its fifth mode, producing a 67.4 dB sound. When the semi-active control is activated, the dominant peak is reduced to 49 dB, as shown in Fig. 13, but the noise is slightly excited at other frequencies. Figure 14 shows the corresponding sound pressure variation in the time domain, showing a significant reduction of the overall sound pressure level as a result of control. Figure 15 shows the voltage on the piezoelectric actuator. Since the waveform of the voltage is very close to sinusoidal signal, the high-order harmonic noise is relatively weak in the case. The attenuation of overall sound pressure level is about 17.8 dB, which is much better than the first frequency case.

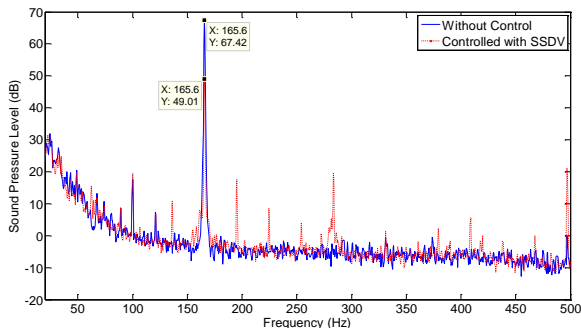


Figure 13 – Spectrum of sound pressure level

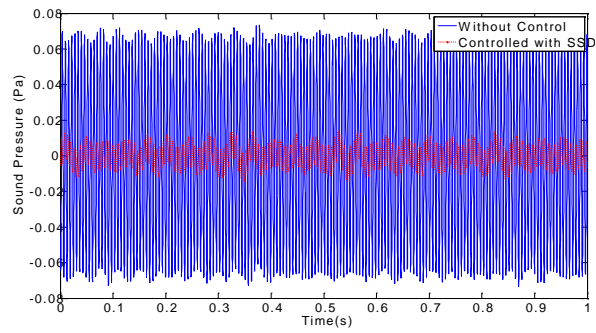


Figure 14 – Sound pressure in time domain

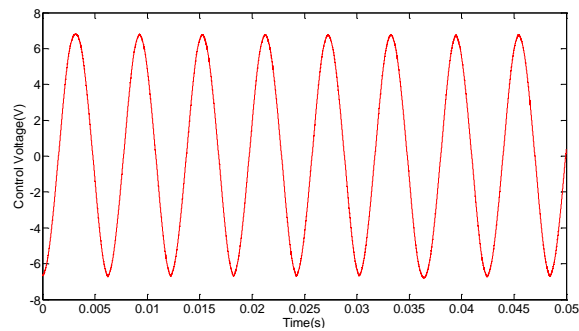


Figure 15 – Voltage on the piezoelectric actuator

5.2 Two-Mode Control

The two-mode control scheme attempts to control both structural modes simultaneously. In the experiments, the panel was excited simultaneously by two harmonic sounds at 52 Hz and 166 Hz. The spectrum of the sound pressure is shown by the solid line in Figure 16. The peaks at the two frequencies of excitation are dominant, but there are also small peaks at other frequencies. In order to control the two components of noise dominated by different structural modes, the piezoelectric patches were divided into two sets and switched by two independent circuits as discussed above. The first set of actuator (the one at the center) was used to target the 5th mode and the second set including a cluster of four PZT patches was used to counter the 1st mode. In order to tackle these two modes, the vibration of the panel is needed. The acceleration of the panel was measured by the accelerometer and modal displacements of the two modes were identified by a state observer [25]. The identified displacements were used for action control of the two switches.

The spectrum of the controlled sound pressure is shown in Figure 16, which shows that the peak at 52 Hz is reduced by 5.2 dB, whilst the one at 166 Hz by 15.8 dB. Figure 17 shows the corresponding sound pressure variation in the time domain. The amplitude of the sound pressure is reduced significantly. An attenuation of 12 dB was achieved in the overall sound pressure level.

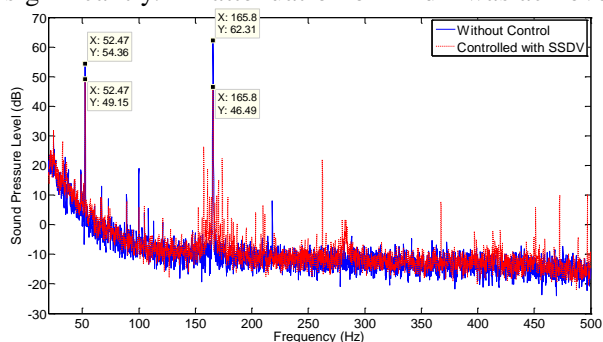


Figure 16 Spectrum of sound pressure level in two-mode control

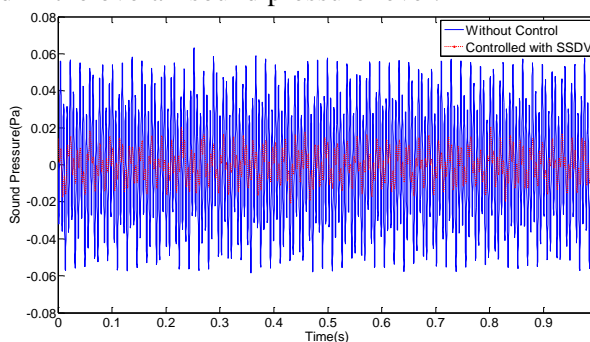


Figure 17 Time history of sound pressure in two-mode control

Having demonstrated the performance of the proposed semi-active SSDV method, a few remarks are noteworthy. Since noise transmission occurs mainly at the resonant frequencies of the panel, it is assumed that suppression of sound transmission can be attributed to the added damping effect through SSDV control. To verify this assumption, the panel vibration was also measured using the accelerometer attached to the panel. Figure 18 shows the spectrum of the acceleration without and with control when the two main modes were excited. It can be seen that the acceleration at 52 Hz was reduced by about 5 dB and that at 166 Hz was reduced by 10 dB. While the reduction levels in both vibration and the radiated sound at the first resonance (52 Hz) are very close (around 5 dB in both cases), the ones at 166 Hz are rather different. In fact, the noise level reduction (15.8 dB) exceeds that of the vibration level (10 dB) by nearly 6dB. This observation surmises that apart from the added damping effect (pertinent to the first resonance frequency), there might be other effects on the structural radiation imposed by the SSDV control. This need to be further clarified by our future work.

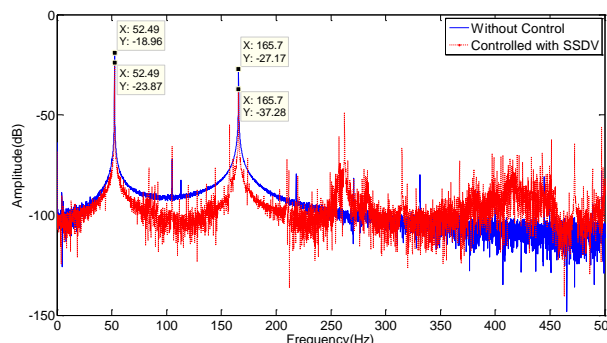


Figure 18 Spectrum of acceleration in two-mode control

The advantage of semi-active SSDV control for suppression of noise transmission is that its

system can be realized without using acoustic sensors for feedback because the voltage inversion is synchronized with vibration so that it can be implemented with strain sensors such as piezoelectric patches. A side effect is that the switched voltage contains high-order harmonic components, which can excite high-frequency vibration and noise. However, the problem can be overcome by increasing the voltage inversion time as illustrated above.

Since sound transmission is mainly induced by resonant vibration in the experimental system of this study, the switches can be directly controlled by the modal displacements, which are identified from the sensor signal using a modal observer. In some systems, strong noise transmission occurs at non-resonant frequencies. In these cases, the acoustic radiation modes should be identified instead of the vibration modes for switch control. Design of appropriate acoustic radiation modal observer from the mathematical relationship between the mechanical modes and acoustic radiation modes will be topic of future work.

6. CONCLUSIONS

The SSDV method has been successfully applied to the suppression of noise transmission through an aluminum panel. The five piezoelectric patches bonded on the panel were divided into two sets and switched by two independent circuits to control the two dominant modes of the panel. In the two mode control scheme, modal displacements were identified by an observer and used for switch control. The transmitted noise was measured by a microphone sensor for the evaluation of control performance. The experimental results show that by switching the voltages on the sets of piezoelectric actuators independently, the resonant peaks of the transmitted sound can be successfully attenuated. Significant reduction of overall sound pressure level was also achieved in both single-mode and two-mode controls. Analyses point at future research directions where SSDV control mechanisms could be fully revealed.

ACKNOWLEDGEMENTS

This research is supported by the NSFC under Grant 51375228, Aeronautical Science Fund under Grant 20131552025, NSF of Jiangsu Province under Grant BK20130791, The State Key Laboratory Program under Grant MCMS-0514K01, the Fundamental Research Funds for the Central Universities under Grant NJ20140012, and PAPD.

REFERENCES

1. Wang XN. Choy YS. Cheng L. Hybrid Noise Control in a Duct Using Light Micro-perforated Plate, *J. Acoust. Soc. Am.* 2012; 132(6): 3778-3787
2. Wang YF. Wang DH. Chai TY. Active control of friction-induced self-excited vibration using adaptive fuzzy systems, *J. Sound Vib.* 2011; 330(17): 4201-4210
3. Yuan M. Qiu JH. Ji HL. et al. Active control of sound transmission using a hybrid/blind decentralized control approach, *Journal of Vibration and Control*, doi: 10.1177/1077546313514758
4. Delany ME. Bazley EN. Acoustical properties of fibrous absorbent materials, *Applied Acoustics*, 1970; 3(2): 105-116
5. Ekici B. Kentli A. Kucuk H. Improving sound absorption property of polyurethane foams by adding tea-leaf fibers, *Archives of Acoustics* 2012; 37(4): 515-520
6. Jones JD. Fuller CR. Reduction of interior sound fields in flexible cylinders by active vibration control, *Journal of Modal Analysis*, 1989; (5): 45-50
7. Petitjean B. Legrain I. Active control experiments for acoustic radiation reduction of a sandwich panel: feedback and feedforward investigations, *Journal of Sound and Vibration* 2002; 252 (1): 19-36
8. Koshigoe S., et al., Active Noise Control Using Neural Network, *Trans. of JSME, Ser. C*, 1998; 64(620): 1333-1338
9. Ho, S., Matsuhisa, H. and Honda, Y., Active Control of Plate-through Noise Transmission, Dynamics and Design Conference 2000, JSME, CD-ROM Proceedings, Paper No. 746
10. Hong, J., et al., Active control of radiated sound from a vibrating plate. In: ASME, VIB-21481. 2001
11. Qiu J. Haraguchi M. Vibration Control of a Plate Using a Self-Sensing Actuator and an Adaptive Control Approach, *Journal Intelligent Material Systems and Structures* 2006; 17(8-9): 661-669
12. Chandra N. Raja S. Nagendra Gopal KV. Vibro-acoustic response and sound transmission loss analysis of functionally graded plates, *Journal of Sound and Vibration*, 2014; 333: 5786-5802
13. Ji HL. Qiu JH. Zhu KJ. Matsuta K. An improved system of active noise isolation using a self-sensing

- actuator and neural network, *Journal of Vibration and Control* 2009; 15(12): 1853-1873
14. Wang KW. Lai JS. Yu WK. Energy-based parametric control approach for structural vibration suppression via semi-active piezoelectric networks, *J VIB ACOUST.* 1996; 115: 505-509
 15. Clark WW. Semi-active vibration control with piezoelectric materials as variable stiffness actuators, In: 1000 AIAA/ASME/ASCE/AHS/ASC Structures, Structural Dynamics, and Materials Conference and Exhibit, 1999, 2623-2629
 16. Richard C. et al., Semi-passive damping using continuous switching of a piezoelectric device, In: SPIE Smart Structures and Materials Conference: Passive Damping and Isolation, 1998, 104-111
 17. Onoda J. Makihara K. Minesugi K. Energy-recycling semi-active method for vibration suppression with piezoelectric transducers, *AIAA Journal*, 2003; 41(4): 711-719
 18. Badel A. et al., Piezoelectric vibration control by synchronized switching on adaptive voltage sources: Towards wideband semi-active damping, *J ACOUST SOC AM*, 2006; 119(5): 2815-2825
 19. Ji HL. Qiu JH. Badel A. Zhu KJ. Semi-active vibration control of a composite beam using an adaptive SSDV approach, *Journal of Intelligent Material Systems and Structures*, 2009; 20(3): 401-412
 20. Yan LJ. Lallart M. Guyomar D. Multimodal nonlinear damping technique using spatial filtering, *Journal of Intelligent Material Systems and Structures*, 2014; 25(3): 308-320
 21. Makihara K. Miyakawa T. Onoda J. Minesugi K. Fuselage panel noise attenuation by piezoelectric switching control, *Smart Materials and Structures*, 2010; 19(8): 085022 (10pp)
 22. Ji HL. Qiu JH. Zhu KJ. Badel A. Two-mode vibration control using nonlinear synchronized switching damping based on the maximization of converted energy, *J. Sound Vib.* 2010; 329: 2751-2767
 23. Fahy F. *Sound and Structural Vibration*, 1985; Academic Press, London
 24. Qiu J. Tani J. and Haraguchi, M. Suppression of Noise Radiation from a Plate Using Self-Sensing Actuators, *Journal Intelligent Material Systems and Structures*, 2005; 16(11-12): 963-970
 25. Ji HL. Qiu JH. Nie H. Cheng L. Semi-active vibration control of an aircraft panel using synchronized switch damping method, *INT J APPL ELECTROM*, 2014, doi: 10.3233/JAE-140096